Original Article

Innate Immunity

Innate Immunity
2014, Vol. 20(5) 529–539

DOI: 10.1177/1753425913501706
ini.sagepub.com
SAGE

MyD88 mediates the decision to die by apoptosis or necroptosis after UV irradiation

Erin Harberts[1], Rita Fishelevich[2], Juan Liu[2], Sergei P Atamas[3,4] and Anthony A Gaspari[1,2]

Abstract

UV irradiation-induced cellular damage is classically associated with apoptosis and is known to result in systemic immunosuppression. How the decision to undergo apoptosis is made following UV is not fully understood. We hypothesize that a central mediator of TLR signaling, MyD88, determines cell fate after UV exposure. Survival after UV of immortalized bone marrow-derived macrophages (BMDM) and *ex vivo* peritoneal macrophages (PM) from MyD88 germline-deficient mice (MyD88$^{-/-}$) was significantly higher than wild type (WT) PM. UV-induced apoptosis (DNA laddering) in PM and epidermis of MyD88$^{-/-}$ animals versus WT was decreased. In MyD88$^{-/-}$ PM, decreased cleavage of caspase 3, as well as pro-necroptotic protein, RIP1, and a significant increase in transcription and release of pro-inflammatory TNF-α, suggest that necroptosis, rather than apoptosis, has been initiated. *In vivo* studies confirm this hypothesis after UV, showing low apoptosis by TUNEL and inflammation in MyD88$^{-/-}$ skin sections. Considering that MyD88 participates in many TLR pathways, BMDM from TLR2$^{-/-}$, TLR4$^{-/-}$ and WT mice were compared for evidence of UV-induced apoptosis. Only TLR4$^{-/-}$ BMDM and PM had a similar phenotype to MyD88$^{-/-}$, suggesting that the TLR4–MyD88 axis importantly contributes to cell fate decision. Our study describes a new cellular consequence of MyD88 signaling after UV, and may provide rationale for therapies to mitigate UV-induced immunosuppression.

Keywords

MyD88, ultraviolet irradiation, apoptosis, necroptosis, TLR4

Date received: 15 February 2013; revised: 30 May 2013; accepted: 24 July 2013

Introduction

Human skin is routinely exposed to UV irradiation, which is a potent immunosuppressant and leads to the apoptosis of resident epidermal cells.[1,2] Apoptotic keratinocytes (KC) that have been irreversibly damaged, termed 'sunburn cells', are sloughed off and replaced.[3] This replacement of epidermal cells by apoptosis allows an intact skin barrier to be maintained with a mild controlled inflammation, and without the intense and exacerbated inflammation associated with other forms of cell death.[4,5] The consequences of not being able to undergo homeostatic apoptosis are highlighted by the recent finding that Fas-associated protein with death domain (FADD)$^{-/-}$ mice, which have a defect in apoptosis, show spontaneous epidermal KC necroptosis and subsequent pathogenic inflammation.[6]

Activation of classical apoptotic pathways leads to a non-inflammatory cell death that results in cleavage and activation of caspase-3. Caspase-activated DNase (CAD) is subsequently cleaved and then translocates into the nucleus to digest genomic DNA, among other cellular components, that is blebbed off in apoptotic bodies. This digestion by CAD results in the DNA laddering that is a hallmark of apoptotic cells.[7] In addition to active cleavage of DNA, apoptotic cells

[1]Department of Molecular Microbiology and Immunology, University of Maryland, Baltimore, MD, USA
[2]Department of Dermatology, University of Maryland, Baltimore, MD, USA
[3]Department of Medicine, University of Maryland, Baltimore, MD, USA
[4]VA Medical Center, Baltimore, MD, USA

Corresponding author:
Anthony A Gaspari, Department of Molecular Microbiology and Immunology, University of Maryland, 410 W. Redwood St., Baltimore, MD 21201, USA.
Email: agasp001@umaryland.edu

undergo loss of survival signals and homeostatic processes. Experiments using caspase inhibitors show that in the absence of the ability to activate the apoptotic pathway, cell death can be skewed to an inflammatory, caspase-independent cell death termed necroptosis.[8]

Necroptosis, a variant of necrosis, is initiated by a RIP1–RIP3 protein complex and leads to inflammatory cell death.[9–11] The consequences of, and cellular mechanisms leading to, the formation of the RIP1–RIP3 protein complex, and subsequent necroptosis, is still an active area of investigation. RIP1 is known to be cleaved and rendered inactive during apoptosis, absence of this RIP1 cleavage and an increase in RIP3 are now identified as markers of necroptosis.[12,13] The recently reported ability of RIP1 to mediate production of TNF-α during necroptosis helps describe the inflammatory nature of necroptotic cell death and may prove to also be a hallmark of necroptosis.[14] Furthermore, TNF-α is up-regulated in both human and mouse skin in response to UV irradiation, and subsequent signaling through the TNF receptor can lead to multiple types of cell death.[15] These deaths can be either caspase-dependent (apoptotic), or caspase-independent (necrotic), and this cell fate decision is shown to be dependent on the levels of active RIP1 and RIP3 in the cell.[16–18] Many inflammatory and necrotic phenotypes have been reported as a result of inhibiting the apoptosis pathway components. For example, mice in which caspase-8 is conditionally deleted in hepatic cells die of necrosis of the liver.[19] Also, intestinal epithelial cell FADD conditional knockout mice develop a spontaneous colitis phenotype that is rescued when RIP3 is also knocked out.[20] Previously described inflammatory phenotypes may now be better explained as a consequence of using necroptosis as a default death pathway when apoptosis is inhibited.

MyD88 is a protein that contains a Toll-IL-1R resistance (TIR) domain on its C-terminus and a death domain on its N-terminus, and is best known for its role as a necessary scaffolding protein in most of the TLR and IL-1 family signaling pathways.[21] It has been reported that MyD88 is capable, upon TLR2 activation, of scaffolding with FADD and initiating a non-traditional extrinsic apoptotic cell death.[22,23] It has also been shown that over-expression of MyD88 alone, but not a control protein, can cause spontaneous apoptosis.[24]

The apoptotic and immunosuppressive effect of UV irradiation on skin suggests that immunomodulatory molecules are activated in epidermal cells upon UV exposure. However, these specific signaling molecules and pathways have yet to be elucidated. It has been found that TLR4 plays a role in promoting cutaneous immunosuppression, as TLR4$^{-/-}$ mice are resistant to the loss of contact hypersensitivity reactions after UV exposure typically observed in susceptible strains of wild type (WT) mice.[2] This TLR4-driven resistance to immunosuppression has been attributed to increased T-regulatory cell function.[2,25] Expression of TLRs 2 and 4 has also been shown to be increased in epidermal cells following UV, and an observed increase in immune signaling molecules, such as MAPK and NF-κB, is dependent on TLR expression.[26] Upon incubation with UV-irradiated KC, these signaling molecules are also up-regulated in Langerhans cells, skin-resident APC, which is dependent on TLRs 2 and 4.[27] Low-dose UV has also been shown to lower the threshold for TNF-related apoptosis-inducing ligand (TRAIL)-induced apoptosis in KC.[28] The importance of TLR signaling in the cutaneous immunomodulatory effect of UV and advances in the understanding of the interconnectedness of cell fate pathways led us to investigate how TLR signaling and the pathway scaffolding adaptor protein, MyD88, may affect cell fate after UV irradiation. In this study, we report that the MyD88–TLR4 signaling axis plays a role in initiating apoptosis after UV irradiation, and without MyD88, UV-induced cell death is skewed to necroptosis.

Materials and methods

Cell culture

Bone marrow-derived macrophages (BMDM) cell lines, utilized in experiments from Figure 1, were derived from MyD88$^{-/-}$ and WT C57BL/6 mice, a generous contribution from Dr Douglas Golenbock (University of Massachusetts Medical School), and were cultured as previously described.[29] Immortalized BMDM from WT, TLR2$^{-/-}$ and TLR4$^{-/-}$ mice on a C57BL/6 background, utilized in experiments from Figure 5, were obtained from BEI Resources (Manassas, VA, USA) (repository numbers NR-9456, NR-9457 and NR-9458, respectively), and were cultured in DMEM supplemented with 10% FCS, 100 μg/ml Pen-Strep, sodium pyruvate and 200 mM L-glutamine. Peritoneal macrophages (PM) obtained by thioglycollate administration in mouse abdomen were purified by short plastic adherence in culture media, DMEM supplemented with 20% FCS, and 100 μg/ml Pen-Strep, then washed three times and cultured as described for experimental use.

UV light source

Groups of four mice at a time or cell culture plates with the media removed were irradiated with a panel of 122 cm Q-Sun light bank (Q-Panel Laboratory products, Cleveland, OH, USA) (equipped with a UVC WG320 filter) at a distance of 30 cm from the light source to their shaved abdominal skin. The spectral emission profile of this light source closely mimics that of natural sunlight, emitting predominantly

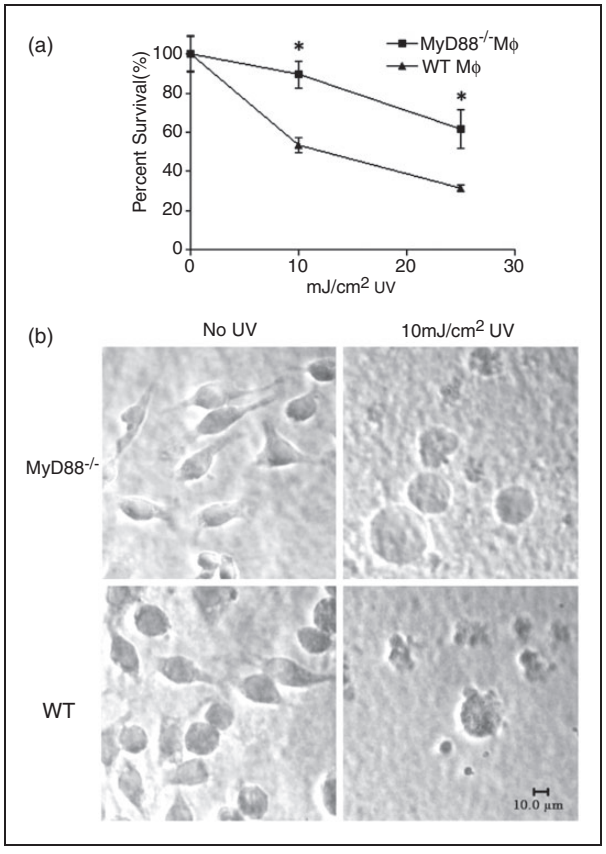

Figure 1. UV-irradiated MyD88$^{-/-}$ cell line has increased survival and decreased apoptotic morphology. (a) Percentage survival of immortalized BMDM from WT C57BL/6 and MyD88$^{-/-}$ mice is measured 24 h after UV using an MTT assay; mean of six replicates $\pm$ SD is shown. Percentage survival is normalized to un-irradiated control. A significant difference ($^{*}P < 0.0001$) in survival is seen at both UV doses (10 mJ/cm^2 and 25 mJ/cm^2). (b) The WT and MyD88$^{-/-}$ cell lines are un-irradiated or irradiated with 10 mJ/cm^2 of UV and visualized 24 h after irradiation for signs of apoptotic morphology. WT cells show condensed nuclei and blebbing off of cellular material, MyD88$^{-/-}$ cells appear swollen and show decreased apoptotic morphology. Results are representative of three separate experiments.

UVA. A UVB radiometer (National Biologic, Twinsburg, OH, USA) was used to determine UVB output and to calculate the time necessary to deliver the desired doses of UVB.

DNA extraction and ladder assay

Whole genomic DNA was extracted using DNeasy Blood and Tissue Kit (Qiagen, Germantown, MD, USA) following the manufacturer's protocol. To assay for DNA laddering, 500 ng of DNA was loaded next to a 1-kb DNA ladder (Fermentas cat# SM0313) into a 1.2% agarose gel and electrophoresed at 100 V for 10 min followed by 70 V for 60 min. The gels were then stained with ethidium bromide and visualized using ChemiDoc XRS (BioRad, Hercules, CA, USA).

RNA extraction and real-time PCR

RNA extraction, cDNA synthesis kit, and real-time PCR (qPCR) were run according to previously published methods.[30,31] Relative levels of TNF-α mRNA were normalized to 18S mRNA. Primers used in the reactions were purchased from Qiagen, TNF: NM_013693.2 (reference position: 857-879); 18s: X03205.1 (reference position: 1447).

MTT assay

BMDM cell lines or primary KC cells were cultured in a 96-well plate in six replicates, then irradiated with UV as indicated. Twenty-four h after UV irradiation, MTT assay was completed as previously described.[32]

In vivo *experiments*

Mouse experiments were approved by University of Maryland, Baltimore Institutional Animal Care and Use Committee (IACUC). Hair was removed from the abdomen of 14–16-wk-old female WT C57BL/6 mice (The Jackson Laboratory (Bar Harbor, ME, USA), Strain Name: C57BL/6J, Stock Number: 000664) or MyD88$^{-/-}$ mice on a C57BL/6 background (The Jackson Laboratory (Bar Harbor, ME, USA), Strain Name: B6.129P2(SJL)-*Myd88*$^{tm1.1Defr}$/J, Stock Number: 009088), the abdomen was then exposed to 70 mJ/cm^2 of UVB. Numbers of mice irradiated and samples collected are described in the figure legend associated with each experiment. For skin section staining and epidermal DNA laddering experiments, skin biopsy specimens were taken immediately before and 24 h after UV exposure. Samples for sectioning and staining were placed in formalin, while sections for epidermal DNA extraction were incubated at 37°C for 2 h in Dispase (BD Biosciences (Franklin Lakes, NJ, USA) cat# 354235). The epidermal layer was removed from the dermis then used for genomic DNA extraction. To obtain *ex vivo* peritoneal macrophages, 2 ml of thioglycollate medium (Remel (Lenexa, KS, USA) cat# R064712) was injected i.p. into 6–8-wk-old mice and the peritoneal exudates collected 4 d later. For TLR4$^{-/-}$ PM, 6–8-wk-old mice were purchased (The Jackson Laboratory (Bar Harbor, ME, USA) Strain Name: B6.B10ScN-*Tlr4*$^{lps-del}$/JthJ, Stock Number: 007227).

Protein extraction, Western blots and ELISA

Protein concentration from cell lysates made using RIPA buffer was measured using *DC* protein assay (BioRad). For Western blots, 10 µg of protein per lane was loaded into NuPAGE 10% Bis-Tris gel (Life Technologies (Washington, DC, USA) cat# NP0301), then electrophoresed and transferred to nitrocellulose membranes using the Novex mini-gel system

(Invitrogen, Grand Island, NY, USA). Membranes were then probed with one of the following primary Abs: anti-β-actin polyclonal Ab (Cell Signaling, Danvers, MA, USA, cat# 4967), anti-RIP1 monoclonal Ab (Cell Signaling, Danvers, MA, USA, cat# 3493), anti-RIP3 polyclonal Ab (Santa Cruz, Dallas, TX, USA, cat# sc-47364) and anti-Caspase3 (Cell Signaling cat# 9665). Then membranes were developed using the Western Breeze kit (Invitrogen cat# WB7104 or WB7106) according to the manufacturer's protocol. TNF-α quantification was carried out by the Cytokine Core Laboratory (University of Maryland, Baltimore, MD, USA) using the Luminex Multianalyte Assay.

Immunohistochemistry

Formalin-fixed WT and MyD88$^{-/-}$ mouse skin sections were paraffin-embedded, sectioned and stained using TUNEL In Situ Death Detection kit (Roche (Branford, CT, USA) cat# 11684809910). *Ex vivo* PM were cultured and irradiated with 25 mJ/cm^2 UV in chamber slides, then fixed in paraformaldehyde and stained with 1° Ab for cleaved caspase-3 (Cell Signaling cat# 9664). Slides were then stained with FITC-conjugated 2° Ab (Pierce, Rockford, IL, USA, cat# 31583) for fluorescent visualization. Slides were visualized using a Nikon Eclipse E600 microscope and the images documented using the Spot imaging system (Diagnostic Instruments, Sterling Heights, MI, USA). This microscope was also used to visualize cultured macrophage cell lines for morphology after UV.

Statistics

Quantitative data were analyzed for statistically significant differences, between groups of n replicates as described in the associated figure legend, using GraphPad Instat (GraphPad, San Diego, CA, USA). An ANOVA analysis was applied to the quantitative data with a value of $P < 0.05$ considered significant.

Results

The cellular response leading to apoptosis after UV irradiation is MyD88-dependent

To investigate if MyD88 is involved in the cell fate decision after UV irradiation, immortalized BMDM from WT C57BL/6 mice and MyD88$^{-/-}$ mice were cultured and irradiated with increasing doses of UV. After irradiation, the MyD88$^{-/-}$ cells exhibited significantly increased survival ($P < 0.0001$; Figure 1a). To characterize this phenotype further, morphology of the cell lines was visualized 24 h after UV irradiation. The WT BMDM showed characteristic apoptotic morphology with condensed chromatin and blebbing of cellular material. However, MyD88$^{-/-}$ cells appeared swollen and rounded, and without nuclear chromatin condensation (Figure 1b). The morphologic changes seen in the WT macrophages are characteristic of the non-inflammatory apoptotic cell death associated with UV irradiation, while MyD88$^{-/-}$ cell morphology is consistent with that of a cell undergoing necrosis.

To confirm that these observations hold true *in vivo,* the abdomens of WT and MyD88$^{-/-}$ mice were irradiated with an immunosuppressive dose of UV, and the exposed skin evaluated for signs of apoptosis or necrosis. At 24 h after UV exposure, there were no gross differences (i.e. erythema, scale or eschar) between the appearance of the skin of MyD88$^{-/-}$ mice and that of WT mice. Epidermal genomic DNA extracted from the irradiated skin of WT mice shows evidence of apoptosis in the form of prominent DNA laddering 24 h after irradiation, when UV-induced apoptosis is known to peak. Epidermal DNA from MyD88$^{-/-}$ mice does not show this prominent laddering (Figure 2a). An apoptotic DNA ladder is also present in WT, but absent in MyD88$^{-/-}$ PM examined *ex vivo* 24 h after 25 mJ/cm^2 UV irradiation (Figure 2b). These *ex vivo* MyD88$^{-/-}$ PM also exhibited increased survival after UV when compared with WT PM, with a significant difference observed 24 h after 25 mJ/cm^2 of UV irradiation (Figure 2c). MyD88$^{-/-}$ cells show increased survival and decreased apoptosis after UV irradiation.

To look for further evidence of apoptosis, skin biopsy specimens from un-irradiated and irradiated skin were sectioned and stained with hematoxylin and eosin (H&E) or TUNEL (Figure 3). Un-irradiated skin from both WT and MyD88$^{-/-}$ mice exhibited normal histologic features, and, as expected, no TUNEL-positive cells were observed (Figure 3, top panels). UV-irradiated skin from WT mice maintain an intact epidermis with multiple shrunken, pyknotic KCs scattered throughout the epidermis; TUNEL staining confirmed these were apoptotic KC (Figure 3, third panels). In contrast, the epidermis of UV-irradiated MyD88$^{-/-}$ mice revealed histologic signs of epidermal necrosis. A sheet of eosinophilic staining of the upper epidermis with abnormal retained nuclei indicating necrotic cell death is observed, while having sparse TUNEL positivity (Figure 3, bottom panels). There was no grossly different exaggerated sunburn response in MyD88$^{-/-}$ mice compared with WT mice. These histologic features are consistent with the lack of DNA laddering seen in the epidermal DNA of these MyD88$^{-/-}$ mice, and further contribute to the microscopic and biochemical evidence that MyD88$^{-/-}$ cells are not able to efficiently undergo UV-induced apoptosis.

UV irradiation activates necroptotic cell death pathway in cells lacking MyD88

The proteins RIP1 and RIP3 are thought to be main components of the recently described 'necroptisome'

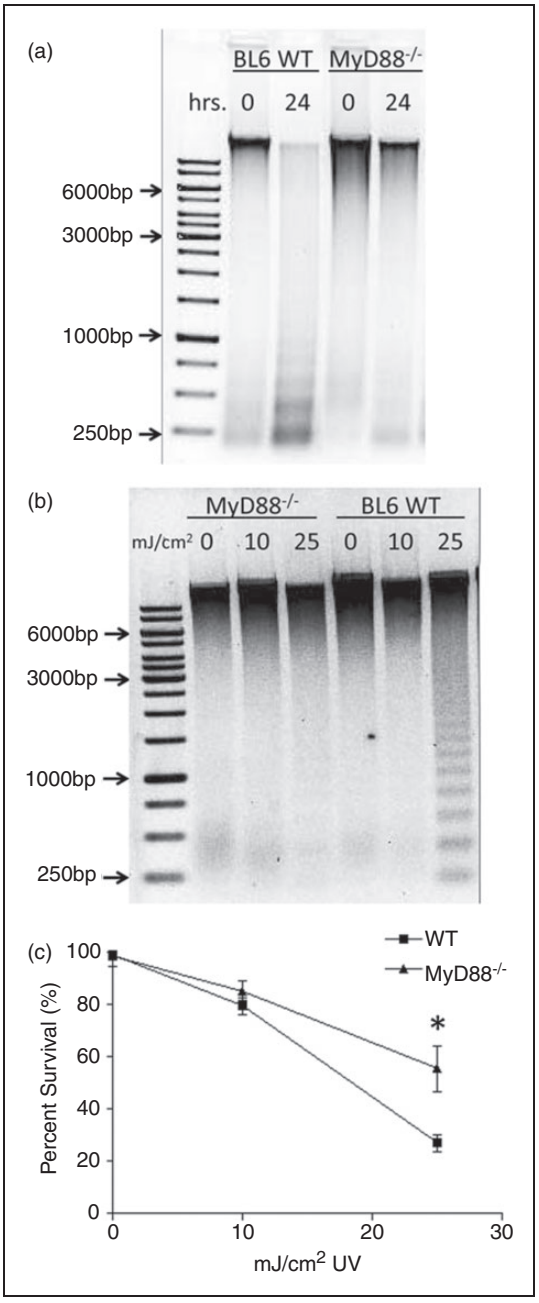

Figure 2. Epidermal DNA from *in vivo* UV-irradiated MyD88$^{-/-}$ mice and *ex vivo* UV-irradiated PM have decreased DNA laddering when compared with WT. (a) Epidermal DNA was extracted from C57BL/6 WT and MyD88$^{-/-}$ abdomen skin biopsies immediately after and 24 h after 70 mJ/cm^2 UV irradiation. To assay for apoptotic laddering, 500 ng of epidermal genomic DNA was electrophoresed on an agarose gel. A gel with DNA from one representative mouse from each group of three is shown. (b) DNA extracted from cultured MyD88$^{-/-}$ and WT PM 24 h after either no UV, or 10 or 25 mJ/cm^2 UV. A prominent ladder is seen in the WT cells that received 25 mJ/cm^2 UV, but not in cells from MyD88$^{-/-}$ mice. Inverted images of ethidium bromide-stained agarose gels are shown in both panels. (c) Survival of WT and MyD88$^{-/-}$ PM 24 h after UV was measured using an MTT assay. At the 25 mJ/cm^2 dose of UV the MyD88$^{-/-}$ PM have significantly increased survival (*$P < 0.0001$) when compared with WT; mean of six replicates ± SD is shown.

that results in an ordered necrotic cell death.[9] To investigate if MyD88$^{-/-}$ cells might be exhibiting a necroptotic cell death, PM from WT and MyD88$^{-/-}$ mice were cultured and *in vitro* UV-irradiated, then 0, 10, 60 and 120 min after UV irradiation levels of RIP1 and RIP3 protein were investigated by Western blot analysis. In WT cells, there was a time-dependent cleavage of RIP1 that is characteristic of apoptosis;[33,34] this cleavage was absent in the MyD88$^{-/-}$ cells (Figure 4a). In WT cells, full-length RIP1 decreases 10 min after UV, consistent with the appearance of cleaved RIP1, and is restored and then augmented 60 and 120 min after UV irradiation. MyD88$^{-/-}$ cells showed little variation in full-length RIP1 protein levels; however, they show an induction of the necroptotic protein RIP3 120 min after UV (Figure 4a), in contrast to WT cells where RIP3 protein levels were consistent throughout time course.

Necroptosis results in an inflammatory cell death that leads to the release of pro-inflammatory cytokines, specifically TNF-α. Supernatants from primary peritoneal macrophages were collected 24 h after *in vitro* UV exposure and assayed by ELISA for TNF-α release. A significant increase in TNF-α release was observed in the MyD88$^{-/-}$ cells, but not in the WT cells ($P = 0.0139$; Figure 4b). To further support this finding, RNA was extracted from UV-irradiated PM and levels of TNF-α mRNA were measured by qPCR. Consistent with the ELISA data, we found that TNF-α mRNA is upregulated to a significantly higher level in MyD88$^{-/-}$ PM when compared with WT ($P < 0.05$; Figure 4c). The lack of RIP1 cleavage, induction of RIP3 and the enhanced release of TNF-α support the hypothesis that the necroptotic pathway, rather than an apoptotic pathway, is activated by UV irradiation in the absence of MyD88.

TLR4$^{-/-}$ and MyD88$^{-/-}$ cells have a similar cell fate phenotype after UV irradiation

To begin to elucidate if this cell death phenotype is a result of activation of the TLR signaling pathways for which MyD88 is a necessary scaffolding protein, immortalized BDMM from WT, TLR2$^{-/-}$ and TLR4$^{-/-}$ mice on a C57BL/6 background were used in cell death assays. In an MTT assay, the TLR4$^{-/-}$ macrophages were found to have significantly increased survival ($P < 0.001$) 24 h after exposure to increasing doses of UV irradiation when compared with both WT and TLR2$^{-/-}$ cells (Figure 5a). This is the same survival phenotype observed in MyD88$^{-/-}$ cells, suggesting that the TLR4 signaling pathway and its components, including MyD88, are mediating cell fate after UV irradiation. This observation is supported by the lack of DNA laddering seen 24 h after UV irradiation in TLR4$^{-/-}$ cells (Figure 5b). While a typical apoptotic DNA ladder was seen at both doses of UV

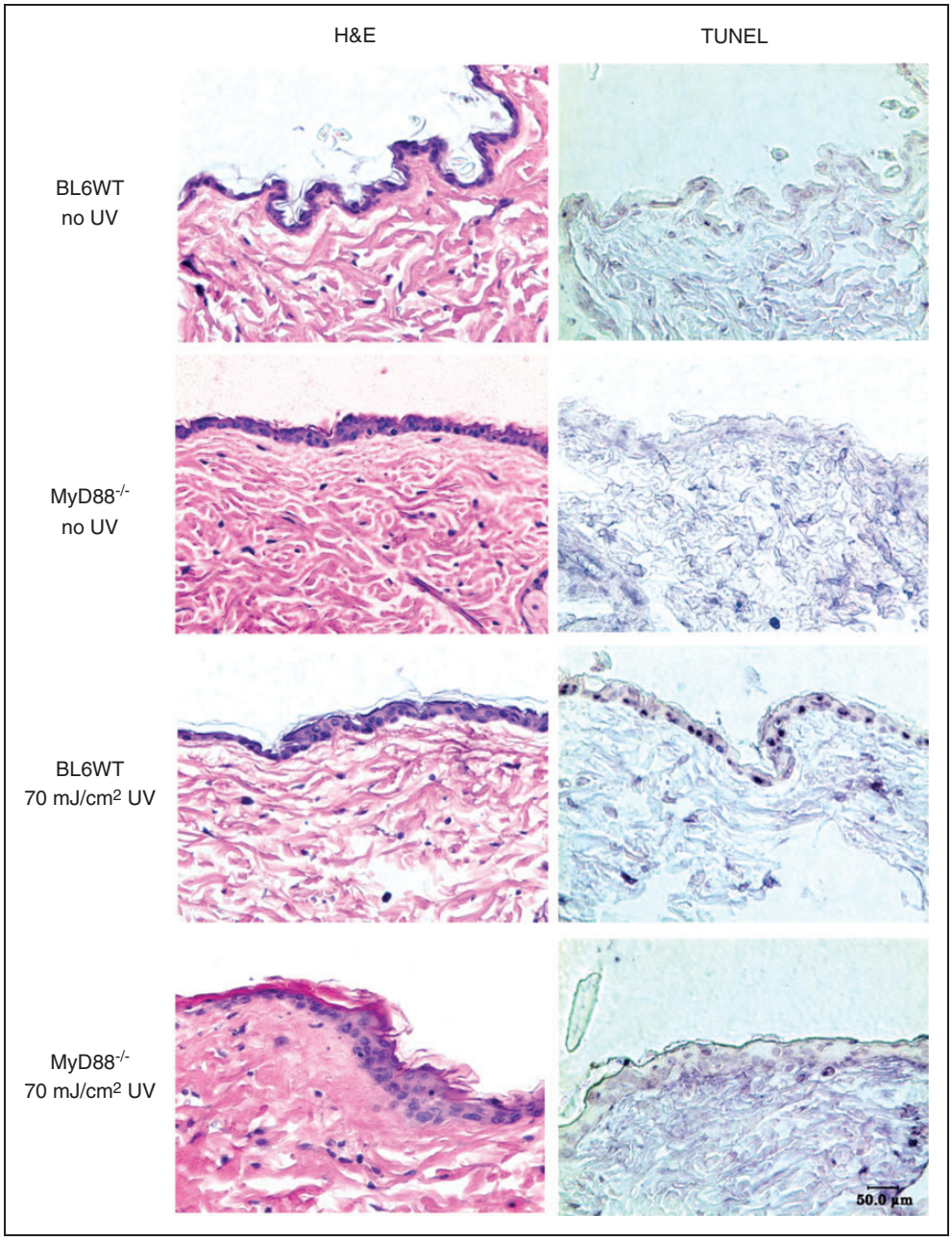

Figure 3. Skin sections from UV-irradiated MyD88$^{-/-}$ mice have decreased epidermal apoptosis and increased evidence of epidermal necrosis than WT. Skin biopsy specimens taken 24 h after UV exposure and un-irradiated biopsies from each group were formalin-fixed and stained with H&E or TUNEL. A representative image from each group of six mice is shown. Only sections from irradiated MyD88$^{-/-}$mice show markedly decreased epidermal cell apoptosis (very rare TUNEL-positive cells), and histologic signs of intense inflammation and possible beginning stages of necrosis (epidermal membrane disappearing, with enlarged undistinguished epidermal cells showing enlarged clear nuclei and DNA, and associated edema and inflammation), while sections from irradiated WT mice show an intact epidermal architecture and a highly TUNEL positive (dark blue) epidermal cells (indicative of nicked dsDNA labeled by TUNEL, suggesting that these cells are undergoing early apoptosis) compared with non-UV epidermal layer and cells (TUNEL-negative).

in the WT and TLR2$^{-/-}$ cells, it was not visible in TLR4$^{-/-}$ cells, even though high doses of UV were used to induce laddering. This evidence supports the hypothesis that the MyD88-dependent TLR4 signaling pathway is contributing to the cell fate decision after UV irradiation.

UV irradiation induced caspase-3 cleavage is dependent on the TLR4-MyD88 signaling axis

To define and characterize the observed UV-induced apoptotic pathway further, cleavage/activation of caspase-3 was investigated in PM from WT, MyD88$^{-/-}$

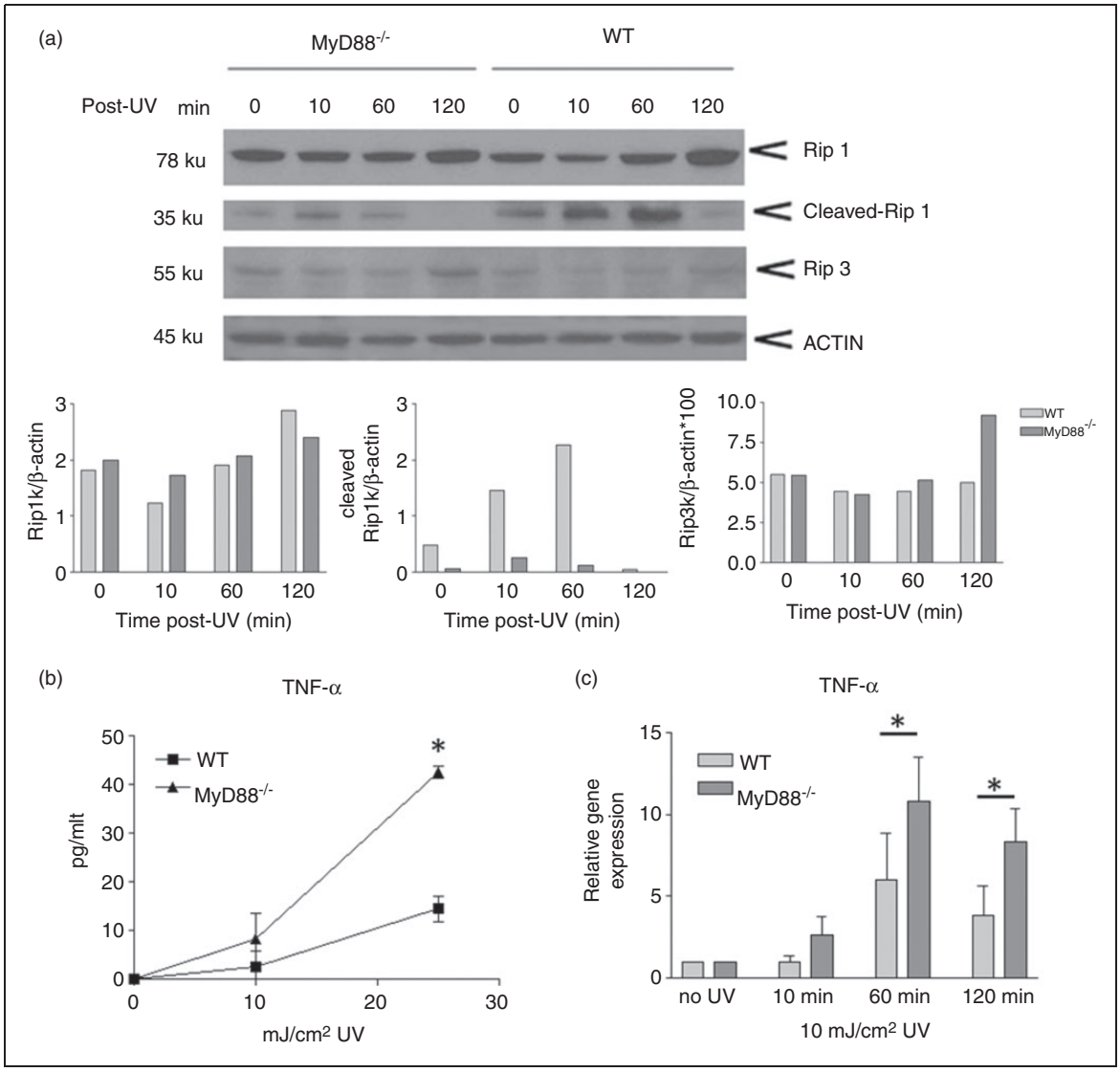

Figure 4. Necroptotic pathway is activated by UV irradiation in MyD88$^{-/-}$ cells. (a) A Western blot of UV-irradiated PM from MyD88$^{-/-}$ or WT mice shows the potential expression kinetics of RIP1, its activation by cleavage and RIP3 expression. Amount of full-length RIP1, cleaved RIP1 and RIP3 are measured by Western blot in WT and MyD88$^{-/-}$ PM. Protein was measured 0, 10, 60 and 120 min after 25 mJ/cm^2 UV. Densitometry-measured relative protein levels normalized to β-actin from a representative of two independent experiments are graphed. These data suggest a potential activation of the necroptosis pathway by UV in MyD88$^{-/-}$ PM. (b) Supernatants from PM cultures were collected 24 h after 0, 10 or 25 mJ/cm^2 UV irradiation, and assayed by ELISA for TNF-α release. The mean ± SD of two independent experiments is shown (*$P = 0.0139$). (c) TNF-α mRNA expression is measured in MyD88$^{-/-}$ and WT PM 0, 10, 60 and 120 min after 10 mJ/cm^2 UV. Significantly greater TNF-α mRNA up-regulation is observed in the MyD88$^{-/-}$ PM compared with WT. The mean ± SD of two independent experiments is shown (*$P < 0.05$).

and TLR4$^{-/-}$ mice. Western blot analysis was carried out with protein lysates collected from cultured WT and MyD88$^{-/-}$ PM 0, 4 and 8 h after 25 mJ/cm^2 UV. There is a time-dependent cleavage of full-length 35-ku caspase-3 into its active 17-ku form in WT cells; however, this cleavage was absent in MyD88$^{-/-}$ cells (Figure 6a). Absence of caspase-3 cleavage in MyD88-deficient cells supports our finding that these cells that lack an intact TLR4 signaling pathway cannot undergo apoptosis after UV irradiation. We also performed immunohistochemistry to stain for cleaved caspase-3 8 h after 25 mJ/cm^2 UV in *in vitro* irradiated PM from WT, MyD88$^{-/-}$ and TLR4$^{-/-}$ cells. Cleaved caspase-3 was visible in the WT culture, but, again, was absent in the MyD88$^{-/-}$ and TLR4$^{-/-}$ cultures (Figure 6b), providing further evidence that the MyD88-dependent TLR4 signaling pathway is necessary for initiation of apoptosis after UV irradiation.

Discussion

In this study we showed that MyD88-deficient mouse immortalized cell lines do not undergo apoptosis efficiently and exhibit increased survival after UV

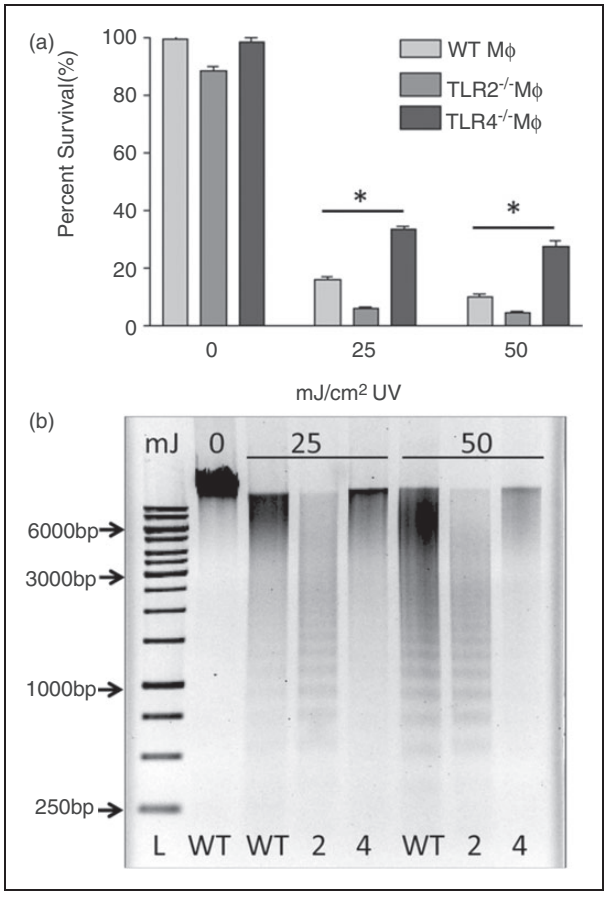

Figure 5. TLR4$^{-/-}$ macrophages exhibit increased survival and decreased apoptosis after UV irradiation. (a) Percent survival of immortalized BMDM from C57BL/6 WT, TLR2$^{-/-}$ and TLR4$^{-/-}$ mice is measured 24 h after 0, 25 or 50 mJ/cm^2 UV using an MTT assay. Mean of six replicates from two independent experiments $\pm$ SD is shown. Percentage survival is normalized to un-irradiated control. When compared with WT and TLR2$^{-/-}$ BMDM, the TLR4$^{-/-}$ BMDM have a significant increase in survival, as measured by MTT assay, at both doses of UV (*$P < 0.001$). (b) Five-hundred ng of genomic DNA extracted from C57BL/6 WT (WT), TLR2$^{-/-}$(2) and TLR4$^{-/-}$(4) immortalized cell lines 24 h after 0, 25 or 50 mJ/cm^2 UV irradiation were electrophoresed on an agarose gel; a 1-kb DNA ladder (L) was included. TLR4$^{-/-}$ DNA does not show a UV-inducible ladder and so is considered not to be apoptotic. Inverted image of ethidium bromide stained agarose gel is shown and is representative of three independent experiments.

irradiation (Figure 1). We then showed that a characteristic apoptotic signature, DNA laddering, is also diminished in *ex vivo* UV-irradiated MyD88$^{-/-}$ mouse epidermal and PM cells, but is present in WT cells (Figure 2). Staining of skin sections from these UV-irradiated MyD88$^{-/-}$ mice shows signs of epidermal necrosis and an absence of TUNEL staining, while WT skin sections show characteristic apoptotic KC after UV irradiation (Figure 3). Although MyD88 is not classically associated with UV-induced apoptosis because this protein contains a death domain, it may be capable of scaffolding with caspase-activating proteins. There are other known mechanisms of UV-induced apoptosis, and so it is interesting, and perhaps surprising, that MyD88 is playing such a critical role in the apoptotic phenotype. FADD is another death domain-containing protein, and has been demonstrated to control the axis between apoptosis and necrosis.[35] Our results suggest that MyD88, like FADD, may play an important role in deciding cell fate after UV irradiation.

Necroptosis is rapidly becoming recognized as an alternative to apoptotic cell death. In this study, we observed activation of necroptotic markers in MyD88$^{-/-}$ cells that are not able to undergo an efficient apoptosis after UV irradiation (Figure 4). Our data are consistent with evolving literature that describes necroptosis as a default cell death pathway in the absence of apoptosis.[1,12,20,36] It has recently been shown that RIP1 controls and induces TNF-α production during necroptosis.[14] We report that after UV irradiation, MyD88$^{-/-}$ cells up-regulate mRNA, and release a significantly increased amount of TNF-α compared with WT cells, which is consistent with necroptotic cell death (Figure 4b, c). This TNF-α release may be acting as a secondary inducer of apoptosis, and may represent an elegant compensatory strategy that the cell has evolved to induce apoptosis in cells in which this pathway has otherwise been inhibited. Increased production of TNF-α may also be contributing to necroptotic cell death, as signaling through the TNF receptor has been shown to induced necroptosis in the presence of RIP3.[18] During studies of glioblastomas it has also been found that TNF-α signaling leads to increased expression of TLR4.[37] Up-regulation of both TNF-α and TLR4, and the positive feedback of one on the other, may contribute to the exacerbated phenotype we observe in our model. Further investigation will be required to further confirm that these MyD88$^{-/-}$ and TLR4$^{-/-}$cells are dying by necroptosis, and to determine the role TNF-α is playing in the necroptotic phenotype observed in this study.

If MyD88 is involved in cell fate secondary to its role as an adapter protein in TLR signaling pathways, then we would expect TLR$^{-/-}$ cells to have a similar phenotype to MyD88$^{-/-}$ cells after UV irradiation. Our data suggest that TLR4, but not TLR2, is involved in the apoptotic response to UV irradiation (Figure 5). The MyD88-dependent TLR4 signaling pathway is specifically necessary for this apoptosis, as the TRIF-dependent TLR4 signaling pathway remains intact in MyD88$^{-/-}$ mice and the necroptotic phenotype is observed. MyD88 has been demonstrated to couple TLR signaling to the caspase-activating, extrinsic apoptotic pathway through its death domain, although specific conditions resulting in this have not yet been elucidated.[23] In this study, we report a lack of caspase-3 activation after UV in both MyD88$^{-/-}$ and TLR4$^{-/-}$ mice (Figure 6). It is possible

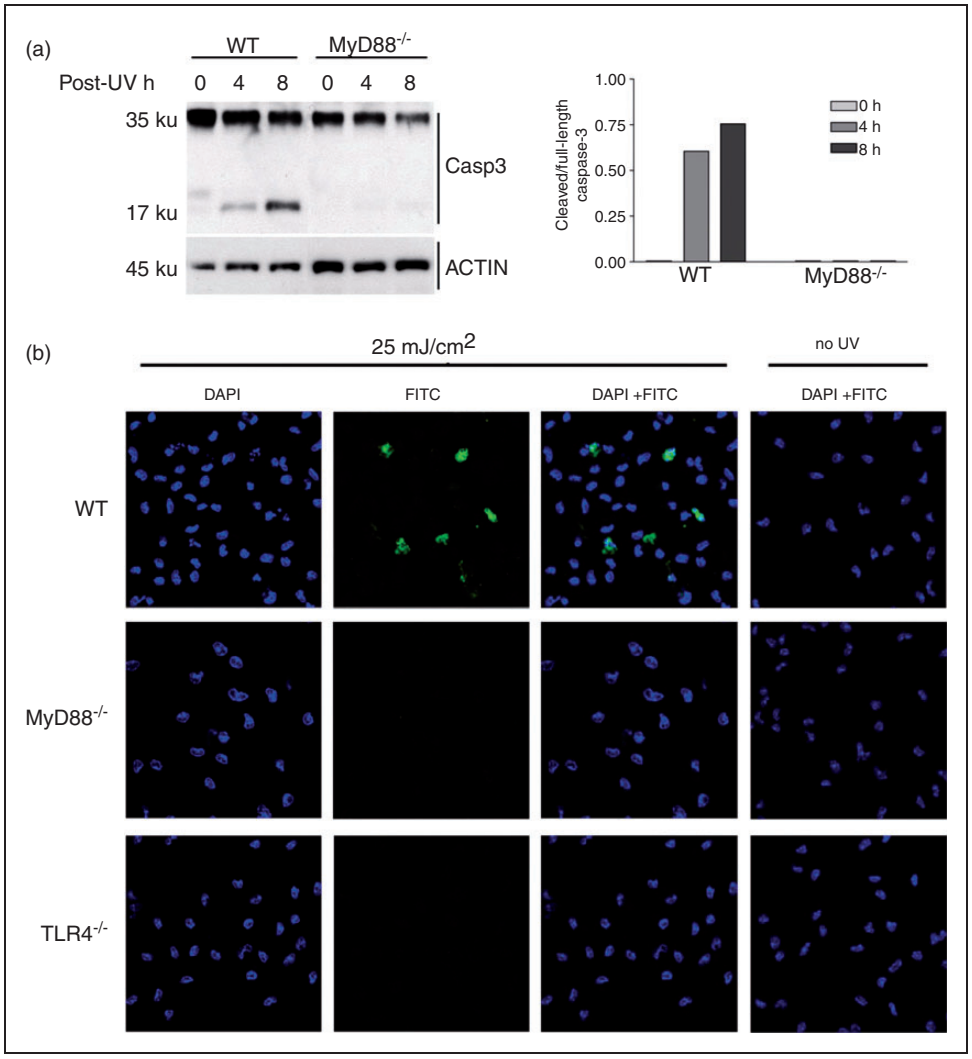

Figure 6. UV-induced caspase-3 cleavage is dependent on the TLR4–MyD88 signaling pathway. (a) Western blot of PM lysates from WT and MyD88$^{-/-}$ mice taken 0, 4 or 8 h after 25 mJ/cm^2 UV irradiation. Blot is probed with a caspase-3 Ab, which shows a 35-ku band representing full-length caspase-3 and a 17-ku band representing the cleaved/activated form of caspase-3, or with a β-actin Ab as a loading control. The activation of caspase-3 by cleavage in WT PM lysates is consistent with apoptosis; the lack of this cleavage in MyD88$^{-/-}$ PM is compatible with the hypothesis of UV-induced necroptosis. Ratio of density of cleaved/full-length caspase-3 is graphed next to image of blot. This blot is a representative of two independent experiments. (b) Cultured PM from WT, MyD88$^{-/-}$ and TLR4$^{-/-}$ mice were fixed 24 h after 25 mJ/cm^2 UV and stained for cleaved caspase-3 (FITC) or with a nuclear stain (DAPI). Globally, DAPI staining is brighter following UV irradiation, and nuclei of MyD88$^{-/-}$ and TLR4$^{-/-}$PM are enlarged compared with those of WT PM (compatible with turgescent cells). In WT PM following irradiation caspase-3 activation by cleavage is observed with FITC in some PM cells at this middle-intensity UV dose, and DAPI staining (left) is lower in these caspase-3-positive cells (observed cell by cell, compatible with ongoing digestion of DNA by caspase-3-activated enzymes CAD; in addition, nuclear fragmentation and condensation can be locally observed). In MyD88$^{-/-}$, as in TLR4$^{-/-}$ PM, no activation of caspase-3 is observed (compatible with no apoptosis); however, at this middle dose, on these micrographs, a clear increase of nuclei size (more than 2×) is observed, with lack of DNA condensation notably in MyD88$^{-/-}$PM nuclei (compatible with the necroptosis hypothesis), and to a minor extent in TLR4$^{-/-}$PM compared with non-UV controls.

that after UV irradiation, TLR4 is activated in a way that allows MyD88 to scaffold with apoptotic proteins as opposed to its classical TLR signaling intermediates. There is also a report that UV irradiation can directly induce ligand-independent trimerization of TNF-α receptor and lead to apoptosis.[38] It will be important in future studies to determine if TLR4 is activated directly by UV irradiation or by a damage-associated molecular pattern released after UV irradiation.

Consistent with our findings, C3H/HeJ mice, which are TLR4-hyporesponsive owing to a spontaneous point mutation in the TLR4 TIR domain that rendered it incapable of signaling in response to TLR4 agonists, exhibit a decreased susceptibility to

UV-induced immunosuppression.[36] Given our findings, we would expect MyD88$^{-/-}$ mice to exhibit a similar phenotype, i.e. decreased UV sensitivity. Perhaps this decreased sensitivity is a result of the lack of apoptotic cell death and subsequent initiation of pro-inflammatory mediators during necroptotic cell death. This hypothesis is supported by the increase in TNF-α mRNA expression and protein release by irradiated MyD88$^{-/-}$ cells (Figure 4b, c). Apoptosis initiated by UV irradiation has long been thought of as a positive consequence that enables the skin to rid damaged cells in a way that does not cause undue inflammation. The immunosuppressive effects of UV irradiation have broad-reaching effects on the immune system, and by allowing cells to die without inflammation, apoptosis caused by signaling through MyD88 may substantially contribute to this impaired immune surveillance.

The skin immune response to UV irradiation has been an active area of investigation with many contributing factors identified. This study reveals a novel role for MyD88-dependent signaling in determining cell fate after UV irradiation, and may provide a rationale for the development of a MyD88-modulating therapy that could potentially be used to mitigate UV-induced immunosuppression.

Acknowledgements

We would like to thank Drs Stefanie Vogel and Robert Ernst, and their laboratory members for helping to review the project and generously donating BMDM cell lines. We also thank Dr Bahram Sina for his help in interpreting the pathology of histologic stains.

Funding

This research was funded by VA Merit Award 1 I01 BX000405-01A2.

Conflict of interest

The authors do not have any potential conflicts of interest to declare.

References

1. Murphy GM. Ultraviolet radiation and immunosuppression. *Br J Dermatol* 2009; 161(Suppl. 3): 90–95.
2. Lewis W, Simanyi E, Li H, et al. Regulation of ultraviolet radiation induced cutaneous photoimmunosuppression by toll-like receptor-4. *Arch Biochem Biophys* 2011; 508: 171–177.
3. Bernerd F, Sarasin A and Magnaldo T. Galectin-7 overexpression is associated with the apoptotic process in UVB-induced sunburn keratinocytes. *Proc Natl Acad Sci U S A* 1999; 96: 11329–11334.
4. Kulms D and Schwarz T. Molecular mechanisms of UV-induced apoptosis. *Photodermatol Photoimmunol Photomed* 2000; 16: 195–201.
5. Lee CH, Wu SB, Hong CH, et al. Molecular mechanisms of UV-induced apoptosis and its effects on skin residential cells: the implication in UV-based phototherapy. *Int J Mol Sci* 2013; 14: 6414–6435.
6. Bonnet MC, Preukschat D, Welz PS, et al. The adaptor protein FADD protects epidermal keratinocytes from necroptosis in vivo and prevents skin inflammation. *Immunity* 2011; 35: 572–582.
7. Widlak P and Garrard WT. Roles of the major apoptotic nuclease-DNA fragmentation factor-in biology and disease. *Cell Mol Life Sci* 2009; 66: 263–274.
8. Vandenabeele P, Vanden Berghe T and Festjens N. Caspase inhibitors promote alternative cell death pathways. *Sci STKE* 2006; 2006: pe44.
9. Han J, Zhong CQ and Zhang DW. Programmed necrosis: backup to and competitor with apoptosis in the immune system. *Nat Immunol* 2011; 12: 1143–1149.
10. Galluzzi L and Kroemer G. Necroptosis: a specialized pathway of programmed necrosis. *Cell* 2008; 135: 1161–1163.
11. Hitomi J, Christofferson DE, Ng A, et al. Identification of a molecular signaling network that regulates a cellular necrotic cell death pathway. *Cell* 2008; 135: 1311–1323.
12. McComb S, Cheung HH, Korneluk RG, et al. cIAP1 and cIAP2 limit macrophage necroptosis by inhibiting Rip1 and Rip3 activation. *Cell Death Differ* 2012; 19: 1791–1801.
13. Rajput A, Kovalenko A, Bogdanov K, et al. RIG-I RNA helicase activation of IRF3 transcription factor is negatively regulated by caspase-8-mediated cleavage of the RIP1 protein. *Immunity* 2011; 34: 340–351.
14. Christofferson DE, Li Y, Hitomi J, et al. A novel role for RIP1 kinase in mediating TNFalpha production. *Cell Death Dis* 2012; 3: e320.
15. Yarosh D, Both D, Kibitel J, et al. Regulation of TNFalpha production and release in human and mouse keratinocytes and mouse skin after UV-B irradiation. *Photodermatol Photoimmunol Photomed* 2000; 16: 263–270.
16. Zhang DW, Zheng M, Zhao J, et al. Multiple death pathways in TNF-treated fibroblasts: RIP3- and RIP1-dependent and independent routes. *Cell Res* 2011; 21: 368–371.
17. Vandenabeele P, Declercq W, Van Herreweghe F and Vanden Berghe T. The role of the kinases RIP1 and RIP3 in TNF-induced necrosis. *Science Signal* 2010; 3: re4.
18. Zhang DW, Shao J, Lin J, et al. RIP3, an energy metabolism regulator that switches TNF-induced cell death from apoptosis to necrosis. *Science* 2009; 325: 332–336.
19. Liedtke C, Bangen JM, Freimuth J, et al. Loss of caspase-8 protects mice against inflammation-related hepatocarcinogenesis but induces non-apoptotic liver injury. *Gastroenterology* 2011; 141: 2176–2187.
20. Welz PS, Wullaert A, Vlantis K, et al. FADD prevents RIP3-mediated epithelial cell necrosis and chronic intestinal inflammation. *Nature* 2011; 477: 330–334.
21. Trinchieri G and Sher A. Cooperation of Toll-like receptor signals in innate immune defence. *Nat Rev Immunol* 2007; 7: 179–190.
22. Aliprantis AO, Yang RB, Weiss DS, et al. The apoptotic signaling pathway activated by Toll-like receptor-2. *EMBOJ* 2000; 19: 3325–3336.
23. Pandey AK and Sodhi A. Recombinant YopJ induces apoptotic cell death in macrophages through TLR2. *Mol Immunol* 2011; 48: 392–398.
24. Jaunin F, Burns K, Tschopp J, et al. Ultrastructural distribution of the death-domain-containing MyD88 protein in HeLa cells. *Exp Cell Res* 1998; 243: 67–75.
25. Dai J, Liu B, Ngoi SM, et al. TLR4 hyperresponsiveness via cell surface expression of heat shock protein gp96 potentiates suppressive function of regulatory T cells. *J Immunol* 2007; 178: 3219–3225.
26. Wang X, Bi Z, Wang Y and Wang Y. Increased MAPK and NF-kappaB expression of Langerhans cells is dependent on TLR2 and TLR4, and increased IRF-3 expression is partially dependent on TLR4 following UV exposure. *Mol Med Rep* 2011; 4: 541–546.

27. Wang XY, Tao CJ, Wu QY and Yuan CD. Protein extract of ultraviolet-irradiated human skin keratinocytes promote the expression of mitogen-activated protein kinases, nuclear factor-kappaB and interferon regulatory factor-3 in Langerhans cells via Toll-like receptor 2 and 4. *Photodermatol Photoimmunol Photomed* 2013; 29: 41–48.
28. Qin JZ, Bacon P, Panella J, et al. Low-dose UV-radiation sensitizes keratinocytes to TRAIL-induced apoptosis. *J Cell Physiol* 2004; 200: 155–166.
29. Hise AG, Daehnel K, Gillette-Ferguson I, et al. Innate immune responses to endosymbiotic Wolbachia bacteria in Brugia malayi and Onchocerca volvulus are dependent on TLR2, TLR6, MyD88, and Mal, but not TLR4, TRIF, or TRAM. *J Immunol* 2007; 178: 1068–1076.
30. Gober MD, Fishelevich R, Zhao Y, et al. Human natural killer T cells infiltrate into the skin at elicitation sites of allergic contact dermatitis. *J Invest Dermatol* 2008; 128: 1460–1469.
31. Fishelevich R, Malanina A, Luzina I, et al. Ceramide-dependent regulation of human epidermal keratinocyte CD1d expression during terminal differentiation. *J Immunol* 2006; 176: 2590–2599.
32. Fishelevich R, Zhao Y, Tuchinda P, et al. Imiquimod-induced TLR7 signaling enhances repair of DNA damage induced by ultraviolet light in bone marrow-derived cells. *J Immunol* 2011; 187: 1664–1673.
33. Vande Walle L, Wirawan E, Lamkanfi M, et al. The mitochondrial serine protease HtrA2/Omi cleaves RIP1 during apoptosis of Ba/F3 cells induced by growth factor withdrawal. *Cell Res* 2010; 20: 421–433.
34. Rebe C, Cathelin S, Launay S, et al. Caspase-8 prevents sustained activation of NF-kappaB in monocytes undergoing macrophagic differentiation. *Blood* 2007; 109: 1442–1450.
35. Lee EW, Kim JH, Ahn YH, et al. Ubiquitination and degradation of the FADD adaptor protein regulate death receptor-mediated apoptosis and necroptosis. *Nat Commun* 2012; 3: 978.
36. Noonan FP and Hoffman HA. Susceptibility to immunosuppression by ultraviolet B radiation in the mouse. *Immunogenetics* 1994; 39: 29–39.
37. Tewari R, Choudhury SR, Ghosh S, et al. Involvement of TNFalpha-induced TLR4-NF-kappaB and TLR4-HIF-1alpha feed-forward loops in the regulation of inflammatory responses in glioma. *J Mol Med (Berl)* 2012; 90: 67–80.
38. Sheikh MS, Antinore MJ, Huang Y and Fornace AJ Jr. Ultraviolet-irradiation-induced apoptosis is mediated via ligand independent activation of tumor necrosis factor receptor 1. *Oncogene* 1998; 17: 2555–2563.